Current Science
CS 5 (5), 4706-4714 (2025)
Received 20 July 2025 | **Revised 15 August** 2025 | **Accepted 16 September** 2025 | **Online Available 08 October** 2025
https://doi.org0/10.52845/CS/2025-5-5-29

Current Science
Current Science

OPEN ACCESS

ISSN(O)2795-8639

Research Article

Scutellarin Improves Insulin Resistance in Rat Skeletal Muscle Cell Lines

Si-li Zheng[1], Biao Fan[2], Xu Xu[3], Chun Liu[3], Shu-de Li[1], Ping Li[4]*, Shao-fang Lin[3]*

[1]Research Platform of the Institute for Neural and Metabolic Diseases, Faculty of Basic Medical Science, Kunming Medical University, Kunming, Yunnan, 650500, China

[2]Department of Cell Biology and Medical Genetics, Institute for Neurological and Metabolic Diseases, Faculty of Basic Medical Science, Kunming Medical University, Kunming, Yunnan, 650500, China

[3]Department of General Practice, Ganmei Hospital Affiliated to Kunming Medical University, Kunming, Yunnan, 650500, China

[4]Department of Pediatrics, the First People's Hospital of Kunming, Kunming, Yunnan, 650500, China

[*]Corresponding Author: Shao-fang Lin, Ping Li

Abstract:

Background: Scutellarin (SCU), the primary active constituent of breviscapine, demonstrates a range of pharmacological properties, including anti-inflammatory, antioxidant, neuroprotective, and circulation-enhancing effects. Previous evidence indicates that SCU can ameliorate insulin resistance (IR). However, the underlying mechanisms through which SCU modulates IR in skeletal muscle cells remain incompletely elucidated.

Methods: The efficiency of lentivirus-mediated IKKβ overexpression was evaluated via immunofluorescence (IF) and Western blot. Cell viability was assessed using the CCK-8. Glucose concentration in the culture medium was determined by the glucose oxidase method. Levels of tumor necrosis factor-α (TNF-α), interleukin-1 (IL-1), and interleukin-6 (IL-6) were quantified using ELISA. mRNA expression of IKKβ and NF-κB-p65 (p65) was detected by RT-qPCR, while protein expression of IKKβ, p65, and phosphorylated NF-κB-p65 (p-p65) was examined using IF and Western blot.

Results: Palmitic acid (PA) treatment successfully induced an IR model in L6 cells. Lentivirus-mediated overexpression of IKKβ, even in the absence of PA, triggered inflammatory responses and metabolic abnormalities resembling the IR phenotype, highlighting the critical role of IKKβ in IR pathogenesis. SCU intervention significantly suppressed the expression of TNF-α, IL-1, and IL-6. Concurrently, both protein and mRNA levels of IKKβ, as well as the phosphorylation level of p65, were markedly downregulated.

Conclusions: SCU inhibits IKKβ expression in skeletal muscle cells, reduces p65 phosphorylation, attenuates inflammatory responses, and consequently improves IR.

Keywords: type 2 diabetes mellitus; insulin resistance; scutellarin; IKKβ/NF-κB-p65

1. Introduction

Insulin resistance (IR) is a pathological condition characterized by reduced responsiveness and sensitivity to the physiological actions of insulin (Elkanawati, et al., 2024; Zhang, et al., 2024), resulting in impaired insulin-mediated glucose uptake and utilization. This condition arises from a combination of genetic, dietary, and environmental factors (Chen, et al., 2023b). IR is a major predisposing factor for type 2 diabetes mellitus (T2DM) (Accili, et al., 2025). The pathogenesis of IR involves functional impairments across multiple tissues and organs, including the liver, adipose tissue, and skeletal muscle (Xourafa, et al., 2024). Among these, defective glucose uptake and utilization in skeletal muscle play a particularly critical role (Khouri, et

al., 2024). Therefore, elucidating the mechanisms governing glucose metabolism in skeletal muscle cells and identifying molecular targets for natural compounds under IR conditions are of significant scientific value for improving IR and advancing the prevention and treatment of T2DM.

Scutellarin (SCU), the principal active component of breviscapine, exhibits diverse pharmacological properties, including anti-inflammatory, antioxidant, neuroprotective, and circulation-enhancing effects (Wen, et al., 2021; Fan, et al., 2023; Chen, et al., 2023a). Studies on IR have indicated that SCU can alleviate IR and improve glucose metabolism by activating both the insulin and AMPK signaling pathways (Gao, et al., 2020). Furthermore, SCU has been reported to ameliorate IR through anti-inflammatory actions mediated via modulation of NF-κB (Ye, et al., 2024). However, it remains unclear whether SCU improves IR specifically by regulating the expression of IκB kinaseβ (IKKβ) and subsequently inhibiting the NF-κB-induced inflammatory response in skeletal muscle cells.

To address this question, this study established a palmitic acid (PA)-induced IR model in L6 skeletal muscle cells. Following lentivirus-mediated overexpression of the IKKβ gene, cells were treated with SCU. The expression of key factors within the IKKβ/NF-κB signaling pathway and the phosphorylation status of associated proteins were detected. This research aims to elucidate the effect and molecular mechanism of SCU on IR in skeletal muscle cells, thereby providing new insights into potential strategies for improving IR.

2. Materials and Methods

2.1 Materials

Cells, drugs, and reagents: SCU (gifted by Professor Chen Peng, School of Pharmacy, Kunming Medical University, purity≥98%); PA (Med Chem Express); rat skeletal muscle cell line (L6 cells, Procell Life Science & Technology Co., Ltd.); fetal bovine serum (FBS) and DMEM medium (Gibco); antibodies against IKKβ, p65, and p-p65 (Proteintech); antibodies against AKT and p-AKT (Cell Signaling Technology); ELISA kits for IL-1, IL-6, and TNF-α (Jiangsu Meimian Industrial Co., Ltd.); reverse transcription kit (Thermo Fisher); lentiviral vector L6-r-ikbkb-3xflag-ZsGreen-PURO (Shanghai Hanheng Biotechnology Co., Ltd.).

2.2 Methods

2.2.1 Cell Grouping and Treatment

L6 cells were divided into the following groups: control, empty vector control (LV-NC), and IKKβ lentiviral overexpression (LV-IKKβ). Cells were cultured in a sterile incubator at 37°C with 5% CO_2, using DMEM medium supplemented with 10% FBS and 1% penicillin-streptomycin. Cells were seeded in 24-well plates at an appropriate density. At 70% confluence, the medium was replaced with DMEM containing 2% FBS to induce differentiation. After approximately 5 days, spindle-shaped myoblasts aggregated and formed bi-nucleated or multi-nucleated myotubes, indicating successful differentiation. Infection efficiency was confirmed by IF and Western blot. Subsequently, different concentrations of PA were applied for 12 h to establish the IR model. Successful modeling was verified by Western blot analysis of AKT and phosphorylated AKT (p-AKT) expression, along with glucose consumption measured via the glucose oxidase method. After successful IR induction, cells were divided into: control group; model group (0.1 mmol/L PA for 12 h, then serum-free medium for 24 h); SCU-30 and SCU-90 groups (0.1 mmol/L PA for 12 h, followed by 0.03 mmol/L or 0.09 mmol/L SCU for 24 h, respectively); LV-IKKβ group (cultured in 10% FBS medium); LV-IKKβ+SCU-30 and LV-IKKβ+SCU-90 groups (treated with 0.03 mmol/L or 0.09 mmol/L SCU for 24 h, respectively).

2.2.2 Cell Viability Assay by CCK-8

L6 cells were seeded in 96-well plates at a density of 1×10^5 cells per well and cultured at 37°C with 5% CO_2. At 70% confluence, the medium was aspirated, and cells were washed three times with sterile 1× PBS. Differentiation was induced using DMEM containing 2% FBS. After approximately 5 days, successful differentiation into myotubes was confirmed. Cells were treated with PA and SCU at various doses and time points. After treatment, CCK-8 reagent was added and incubated for 2 h. Absorbance was measured at 450 nm using a microplate reader, and cell viability was calculated.

2.2.3 Detection of TNF-α, IL-1, and IL-6 Levels by ELISA

Cells were plated in 24-well plates. Following myotube induction as described above and respective group treatments, the culture medium was collected using sterile tubes and centrifuged to obtain supernatant. Levels of TNF-α, IL-1, and IL-6 were determined according to the manufacturer's instructions by measuring absorbance at 450 nm, and concentrations were calculated.

2.2.4 Detection of IKKβ, p65, and p-p65 Protein Levels by Western Blot

A mixed lysis buffer containing protease inhibitor, phosphatase inhibitor, and RIPA lysis buffer was prepared in a 1:1:100 ratio. Cells were lysed using sonication. Protein concentration was determined with a BCA protein assay kit. Proteins were separated by 10% SDS-PAGE and transferred to PVDF membranes via wet transfer. After washing three times with TBST, membranes were blocked with 5% skim milk for 1 h at room temperature. Subsequently, membranes were incubated with primary antibodies (AKT: 1:1,000; p-AKT: 1:1,000; IKKβ: 1:800; p65: 1:600; p-p65: 1:500) overnight at 4°C. After washing, membranes were incubated with secondary antibodies at room temperature for 2 h. Following additional washes, bands were visualized using ECL reagent and detected with a fluorescence chemiluminescence gel imaging system. Band intensity was analyzed using ImageJ software.

2.2.5 Detection of IKKβ, p65, and p-p65 Protein Levels by IF

Cells were seeded on coverslips in 24-well plates. After adherence and treatment, cells were washed three times with ice-cold 1× PBS, fixed with 4% paraformaldehyde for 20 min, and washed again. Permeabilization was performed with 0.5% Triton-X100 for 20 min, followed by three washes. Cells were blocked with 2% BSA for 1 h at room temperature and washed again. Primary antibodies (IKKβ: 1:100; p65: 1:100; p-p65: 1:50) were added and incubated overnight at 4°C. After recovery of the primary antibody and washing, secondary antibodies were applied and incubated in the dark for 1.5 h. Coverslips were mounted using an anti-fade mounting medium containing DAPI. Images were captured with a confocal laser scanning microscope and analyzed using ImageJ.

2.2.6 Detection of IKKβ and p65 mRNA Levels by RT-qPCR

Total RNA was extracted using the Trizol method. RNA purity was assessed spectrophotometrically. cDNA was synthesized using a reverse transcription kit. PCR amplification was performed on a real-time quantitative PCR instrument with specific primers. The reaction mixture contained: 10 μL ROX reagent, 1 μL forward primer, 1 μL reverse primer, 1 μL cDNA, and 7 μL DEPC water. PCR conditions were: 95°C for 2 min; 40 cycles of 95°C for 15s, 61°C for 30s, and 72°C for 20s. GAPDH served as the internal reference, and relative gene expression was calculated using the $2^{-\Delta\Delta CT}$ method. Primers were supplied by Shanghai Generay Biotech Co., Ltd.; sequences are listed in Table 1.

Table1 Primer sequences

Species	genes name	sequences (5'-3')
Rat	IKKβ	F: CGGAACTGGGGGATTTGGAA R: CTGTCGGCATTGCTTGATGG
Rat	NF-κB-p65	F: CCGTGAGGCTGTTTGGTTTG R: GGTCTGCCCTCCTGACTCTA
Rat	GAPDH	F: AGAGACAGCCGCATCTTCTT R: TTCTCAGCCTTGACTGTGCC

2.3 Statistical Analysis

Normally distributed continuous data are expressed as mean ± standard deviation and analyzed using GraphPad Prism 9.5.1. Comparisons between two groups were performed using Student's t-test, while multiple groups were compared using one-way ANOVA. $P<0.05$ was considered statistically significant, and $P<0.01$ indicated high statistical significance.

3. Results

3.1 Detection of Lentiviral IKKβ Overexpression Efficiency and Establishment of the IR Cell Model Using PA in L6 Cells

Compared to the control and LV-NC groups, the

LV-IKKβ group showed significantly increased IKKβ fluorescence intensity and protein expression (P<0.01), confirming successful construction of the IKKβ overexpression model (Figure 1A-D). PA treatment at concentrations exceeding 0.2 mmol/L for over 24 h, and SCU treatment at concentrations above 0.1 mmol/L for more than 48 h, significantly reduced cell viability (Figure 1E, F). The p-AKT/AKT ratio was significantly decreased at PA concentrations of 0.1, 0.2, and 0.4 mmol/L (P<0.01) (Figure 1G, H). Glucose consumption was significantly inhibited in the 0.1-0.4 mmol/L PA groups compared to 0 mmol/L PA (P<0.01) (Figure 1I), indicating successful induction of IR at PA concentrations ranging from 0.05 to 0.4 mmol/L. Based on these results, 0.1 mmol/L PA for 12 h was selected for IR induction, and SCU concentrations of 0.03 mmol/L (30 μmol/L) and 0.09 mmol/L (90 μmol/L) with 24 h treatment were chosen for subsequent experiments.

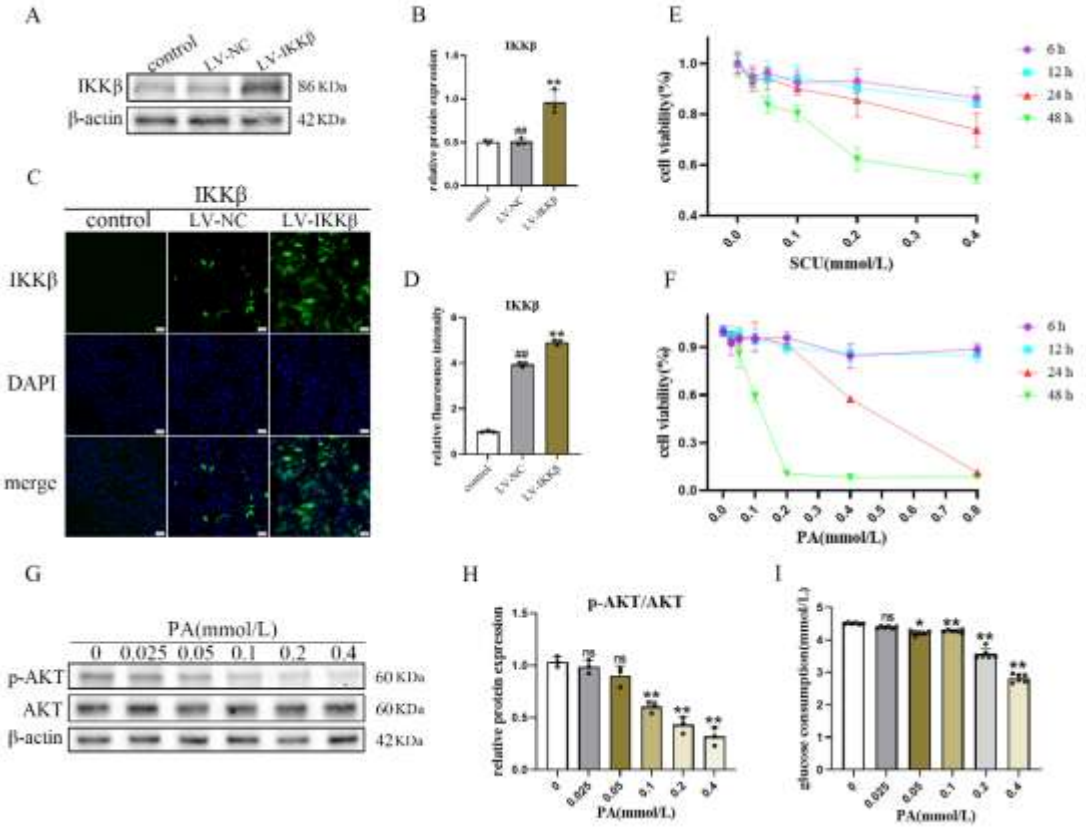

Figure 1 Transfection efficiency of IKKβ lentiviral over-expression in L6 cells and the basis for modelling success in the IR cell model

(A, B) Western blot analysis of IKKβ protein expression and gray value of bands in L6 cells($\bar{x}$±s,n=3); (C, D) IF analysis of fluorescence intensity and optical density values of IKKβ in L6 cells (scale bar is 50 μm,$\bar{x}$±s,n=3); (E) effect of SCU on the viability of L6 cells($\bar{x}$±s,n=4); (F) Effect of PA on the viability of L6 cells($\bar{x}$±s,n=4); (G, H) Western blot analysis of p-AKT/AKT protein expression and gray value of bands in L6 cells($\bar{x}$±s,n=3); (I) glucose oxidase assay for glucose consumption after 12 h treatment with different concentrations of PA($\bar{x}$±s,n=6); **P<0.01 compared with control group; $^{\#\#}$P<0.01 compared with LV-NC group; *P<0.05, **P<0.01 compared with 0 mmol/L.

3.2 SCU Inhibits the Expression of IL-1, IL-6, and TNF-α

Compared to the control group, protein levels of IL-1, IL-6, and TNF-α were elevated in the model and LV-IKKβ groups (P<0.05). SCU-30 and SCU-90 treatments showed decreased protein levels compared to the model group (P<0.05). Similarly, LV-IKKβ+SCU-30 and LV-IKKβ+SCU-90 groups showed decreased protein levels compared to the LV-IKKβ group (P<0.05) (Figure 2A-C).

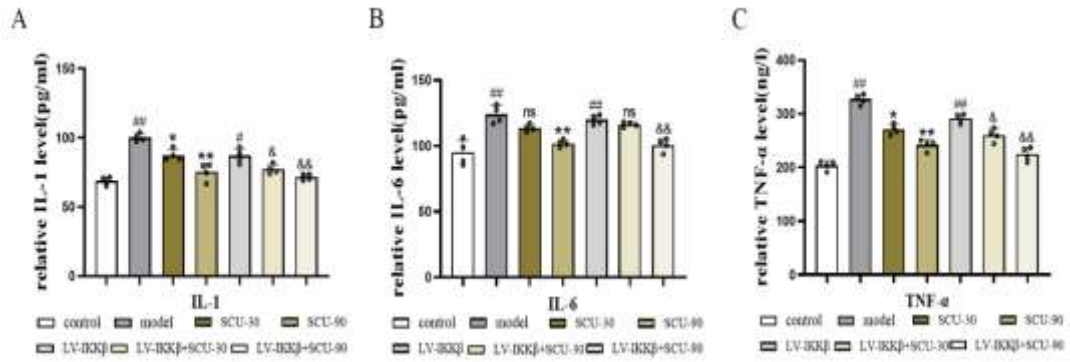

Figure 2 Expression of IL-1, IL-6, and TNF-α in L6 cells(x̄±s,n=4)
(A-C) ELISA kit to detect the expression of IL-1, IL-6 and TNF-α in culture medium in L6 cell; $^{\#}$P<0.05, $^{\#\#}$P<0.01 compared with control group; *P<0.05, **P<0.01 compared with model group; $^{\&}$P<0.05, $^{\&\&}$P<0.01 compared with LV-IKKβ group.

3.3 SCU Inhibits the Expression of IKKβ

IKKβ mRNA and protein expression were significantly increased in the model and LV-IKKβ groups compared to controls (P<0.05). SCU-30 and SCU-90 treatments reduced IKKβ expression compared to the model group (P<0.05). Similarly, LV-IKKβ+SCU-30 and LV-IKKβ+SCU-90 groups showed decreased IKKβ expression compared to the LV-IKKβ group (P<0.05) (Figure 3A-E).

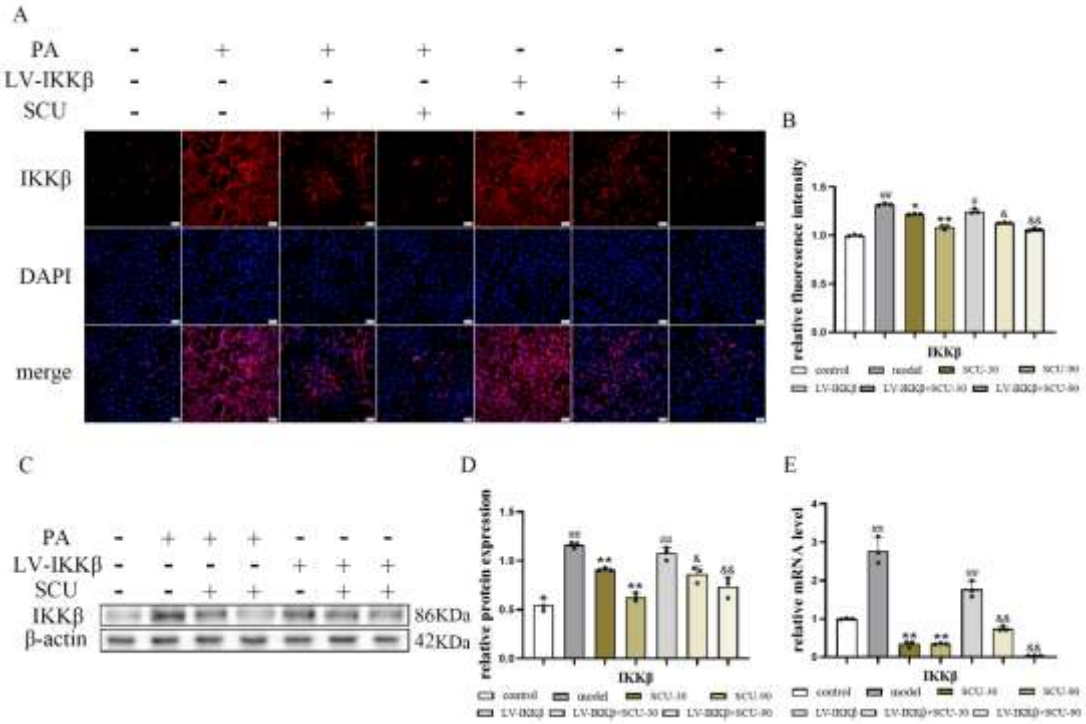

Figure 3 Protein and mRNA expression of IKKβ in L6 cells(x̄±s,n=3)
(A, B) IF analysis of fluorescence intensity and optical density values of IKKβ in L6 cells (scale bar is 50 μm); (C, D) Western blot analysis of IKKβ protein expression and gray value of bands in L6 cells; (E) RT-qPCR analysis of mRNA expression of IKKβ; $^{\#}$P<0.05, $^{\#\#}$P<0.01 compared with control group; *P<0.05, **P<0.01 compared with model group; $^{\&}$P<0.05, $^{\&\&}$P<0.01 compared with LV-IKKβ group.

3.4 SCU Inhibits the Expression of Phosphorylated NF-κB p65 (p-p65)

Protein expression of p-p65 and the p-p65/p65 ratio were significantly increased in the model and LV-IKKβ groups compared to controls (P<0.05). SCU-30 and SCU-90 treatments reduced p-p65 expression and the p-p65/p65 ratio compared to

the model group (P<0.05). Similarly, LV-IKKβ+SCU-30 and LV-IKKβ+SCU-90 groups showed decreased p-p65 expression and p-p65/p65 ratio compared to the LV-IKKβ group (P<0.05) (Figure 4A-G).

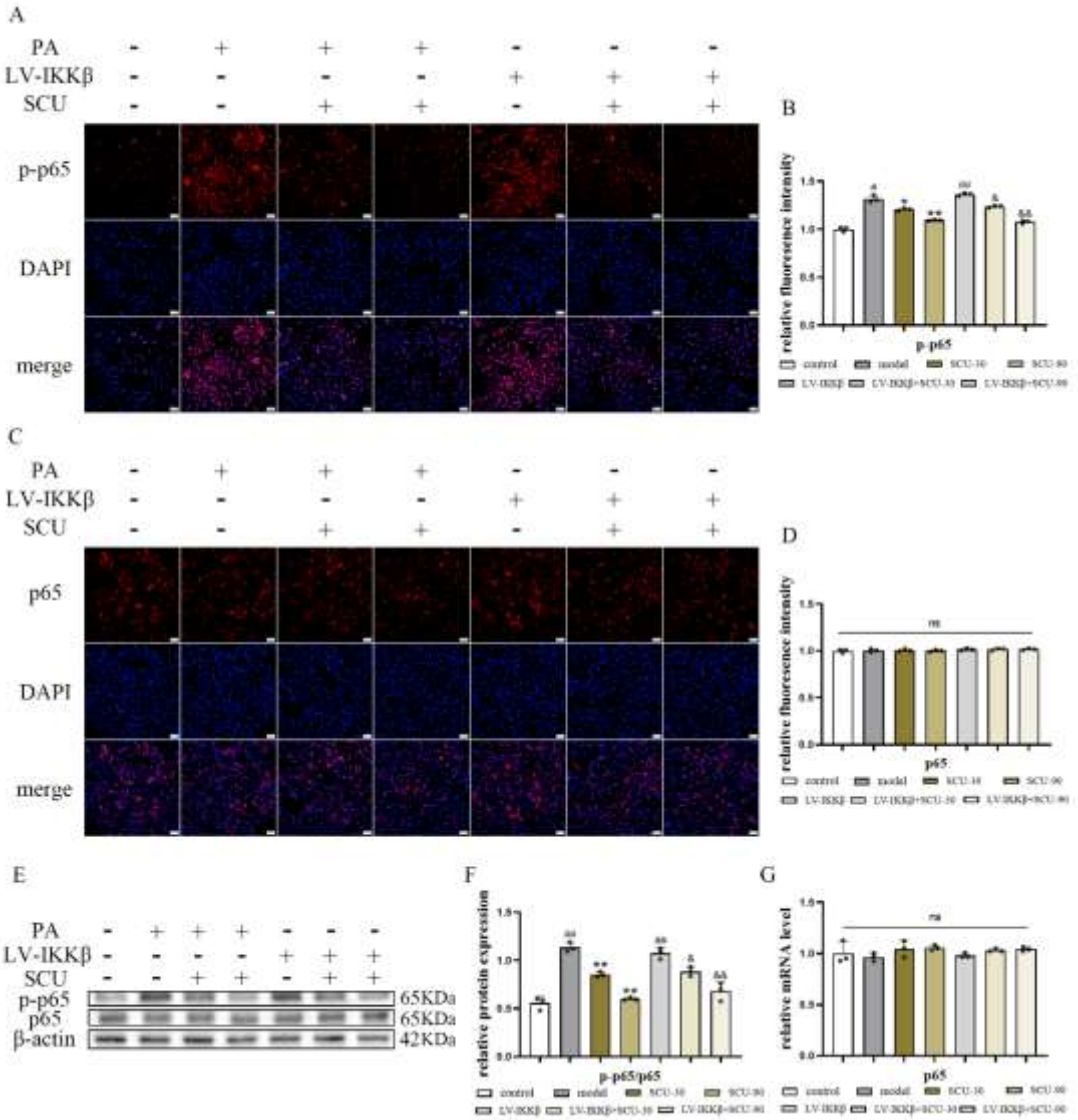

Figure 4 Protein and mRNA expression of p-p65, p65 in L6 cells($\bar{x}$±s,n=3)
(A-D) IF analysis of fluorescence intensity and optical density values of p-p65, p65 in L6 cells (scale bar is 50 μm); (E, F) Western blot analysis of p-p65/p65 protein expression and gray value of bands in L6 cells; (G) RT-qPCR analysis of mRNA expression of p65; $^{\#}$P<0.05, $^{\#\#}$P<0.01 compared with control group; *P<0.05, **P<0.01 compared with model group; $^{\&}$P<0.05, $^{\&\&}$P<0.01 compared with LV-IKKβ group.

4. Discussion

IR is a metabolic disorder characterized by reduced cellular responsiveness to insulin, leading to diminished efficacy in blood glucose regulation (Cheng, et al., 2025). It is a major pathophysiological basis and predisposing factor for T2DM (Ji, et al., 2025). The development of IR is influenced by genetic predisposition, obesity, physical inactivity, poor diet, chronic inflammation, and certain medications (Selman, et al., 2022). Current therapeutic strategies include lifestyle modifications and pharmacological interventions (Jacobo-Tovar, et al., 2025), yet their effectiveness remains limited. This study provides a novel molecular perspective by demonstrating that SCU ameliorates IR in skeletal muscle cells via inhibition of the IKKβ/NF-κB signaling pathway, offering strategic insights for T2DM treatment through SCU-mediated IR

improvement.

IKKβ plays a crucial role in IR development and progression (Den Hartogh, et al., 2025). As the catalytic subunit of the IKK complex, IKKβ activation is a key step in initiating the canonical NF-κB pathway (Li, et al., 2024). Under inflammatory or metabolic stress, IKKβ phosphorylates IκBα at Ser32 and Ser36 (Zhou, et al., 2023), promoting its degradation and enabling NF-κB translocation into the nucleus as p-p65, where it activates transcription of inflammatory mediators (Zhou, et al., 2024a). TNF-α, IL-1, and IL-6, induced by NF-κB activation, form a positive feedback loop that exacerbates local inflammation (Liu, et al., 2025) and systemic IR by promoting adipose tissue remodeling and impairing skeletal muscle glucose uptake (Kuang, et al., 2022). Studies have shown that activation of IKKβ and NF-κB in hepatocytes increases the expression of inflammatory cytokines such as TNF-α, IL-1, and IL-6, thereby worsening IR (Kim, et al., 2023). Thus, targeted inhibition of IKKβ expression or activity holds significant potential for ameliorating IR (Chen, et al., 2025).

Scutellarin (SCU), a natural product, exhibits various biological activities such as anti-inflammatory and antioxidant effects (Zhou, et al., 2024b). Literature reports indicate that in high-fat diet-fed mice and palmitic acid-induced HepG2 cells, SCU reduces hepatic lipid accumulation and ameliorates hepatic IR by regulating the mTOR signaling pathway and suppressing SREBP-1c expression (Luan, et al., 2020). In SD rats, SCU lowers blood glucose, improves IR, and protects renal function through activation of the Nrf2/HO-1 signaling pathway (Younis, et al., 2022). NF-κB is a key factor in inflammatory responses, and Ikkβ activates NF-κB to promote the expression of inflammatory cytokines. As reported, SCU can inhibit IκB degradation and Ikkβ activation, thereby alleviating inflammation and improving IR (Zhang, et al., 2023). These findings further support the conclusion that SCU can ameliorate IR through multiple molecular mechanisms. In this study, PA treatment induced IR in L6 cells, evidenced by elevated inflammatory cytokines and upregulated IKKβ and p-p65 in a dose-dependent manner. High-dose SCU showed superior efficacy. Lentivirus-mediated IKKβ overexpression recapitulated inflammatory and IR characteristics even without PA, underscoring the centrality of IKKβ. SCU intervention suppressed inflammatory cytokines and reduced IKKβ and p-p65 levels dose-dependently, suggesting that SCU may act by directly or indirectly inhibiting IKKβ activity. Notably, SCU reduced p-p65 without affecting total p65, indicating modulation of phosphorylation status rather than total protein expression.

In summary, this study demonstrates for the first time that SCU inhibits IKKβ, reduces p65 phosphorylation, attenuates inflammation, and ameliorates IR in L6 skeletal muscle cells. These findings enhance understanding of SCU's pharmacological actions and provide important theoretical support for its application in alleviating IR and T2DM.

Author Contributions

SFL, PL and SDL designed the research study. SLZ performed the research. BF, XX and CL analyzed the data. All authors contributed to editorial changes in the manuscript. All authors read and approved the final manuscript. All authors have participated sufficiently in the work and agreed to be accountable for all aspects of the work.

Ethics Approval and Consent to Participate

Not applicable.

Funding

This work was supported by grants from the Yunnan Provincial Science and Technology Department (2017FE467(-205)) and the Kunming Health Commission (2022-02-04-001; 2022-SW-28).

Declaration of competing interest

The authors declare that they have no known competing financial interests or personal relationships that could have appeared to influence the work reported in this pape.

Data availability

Data will be made available on request.

References

1. Accili, D., Deng, Z., & Liu, Q. (2025). Insulin resistance in type 2 diabetes mellitus. Nat Rev Endocrinol, 21, 413–426. https://doi.org/10.1038/s41574-025-01114-y
2. Chen, H.-L., Yang, L., Zhang, X.-L.-N., Jia, Q.-Y., Duan, Z.-D., Li, J.-J., Zheng, L.-Y., Liu, T.

-T., Qi, Z., Yuan, Y., & Wu, C.-Y. (2023a). Scutellarin acts via mapks pathway to promote m2 polarization of microglial cells. Mol Neurobiol, 60, 4304-4323. https://doi.org/10.1007/s12035-023-03338-3

3. Chen, Q., Chen, W., Zhang, B., Xue, L., Li, F., Zhang, L., Tong, H., & Zhu, Q. (2025). Hesperetin mitigates adipose tissue inflammation to improve obesity-associated metabolic health. Int Immunopharmacol, 149, 114211. https://doi.org/10.1016/j.intimp.2025.114211
4. Chen, X., Liu, Z., Liu, W., Wang, S., Jiang, R., Hu, K., Sheng, L., Xu, G., Kou, X., & Song, Y. (2023b). Nf-κb-inducing kinase provokes insulin resistance in skeletal muscle of obese mice. Inflammation, 46, 1445-1457. https://doi.org/10.1007/s10753-023-01820-7
5. Cheng, Y., Wu, J., Gao, Y., Ang, B., Chen, Q., Wang, Z., Zeng, M., Qin, F., Chen, J., He, Z., & Wu, F. (2025). Microbial fermentation-derived dihydroquercetin derivatives exhibit superior efficacy in ameliorating insulin resistance via jnk/pi3k/akt pathway regulation compared to dihydroquercetin. J Agric Food Chem, 73, 8323-8337. https://doi.org/10.1021/acs.jafc.5c00109
6. Den Hartogh, D.J., MacPherson, R.E.K., & Tsiani, E. (2025). Muscle cell palmitate-induced insulin resistance, jnk, ikk/nf-κb, and stat3 activation are attenuated by carnosic and rosmarinic acid. Appl Physiol Nutr Metab, 50, 1-14. https://doi.org/10.1139/apnm-2024-0302
7. Elkanawati, R.Y., Sumiwi, S.A., & Levita, J. (2024). Impact of lipids on insulin resistance: Insights from human and animal studies. Drug Des Devel Ther, 18, 3337-3360. https://doi.org/10.2147/DDDT.S468147
8. Fan, X., Wang, Y., Li, X., Zhong, T., Cheng, C., & Zhang, Y. (2023). Scutellarin alleviates liver injury in type 2 diabetic mellitus by suppressing hepatocyte apoptosis in vitro and in vivo. Chin Herb Med, 15, 542-548. https://doi.org/10.1016/j.chmed.2023.03.007
9. Gao, L., Tang, H., Zeng, Q., Tang, T., Chen, M., & Pu, P. (2020). The anti-insulin resistance effect of scutellarin may be related to antioxidant stress and ampkα activation in diabetic mice. Obes Res Clin Pract, 14, 368-374. https://doi.org/10.1016/j.orcp.2020.06.005
10. Jacobo-Tovar, E., Medel-Sánchez, A., Durán-Castillo, C., & Guardado-Mendoza, R. (2025). Insulin resistance in cancer risk and prognosis. Semin Cancer Biol, 114, 73-87. https://doi.org/10.1016/j.semcancer.2025.06.006
11. Ji, H., Su, S., Chen, M., Liu, S., Liu, S., & Guo, J. (2025). Frontiers | the role of gut microbiota in insulin resistance: Recent progress. Front. Microbiol., 16. https://doi.org/10.3389/fmicb.2025.1633029
12. Khouri, H., Roberge, M., Ussher, J.R., & Agueir, C. (2024). Acetoacetate and d- and l-β-hydroxybutyrate have distinct effects on basal and insulin-stimulated glucose uptake in l6 skeletal muscle cells. Am J Physiol Cell Physiol, 326, C1710-C1720. https://doi.org/10.1152/ajpcell.00718.2023
13. Kim, S.-H., Jung, D.-E., Song, J.Y., Jung, J., Jung, J.-K., Lee, H., Roh, E., Hong, J.T., Han, S.-B., & Kim, Y. (2023). Targeting ikkβ activity to limit sterile inflammation in acetaminophen-induced hepatotoxicity in mice. Pharmaceutics, 15, 710. https://doi.org/10.3390/pharmaceutics15020710
14. Kuang, Q.-X., Li, Q.-Z., Lei, L.-R., Wang, Y.-M., Huang, L.-J., Dai, Y.-F., Peng, W., Zhang, M.-Z., Wang, D., Gu, Y.-C., Deng, Y., & Guo, D.-l. (2022). Proliferatins suppress lipopolysaccharide-induced inflammation via inhibition of the nf-κb and mapk signaling pathways. Bioorg Chem, 124, 105810. https://doi.org/10.1016/j.bioorg.2022.105810
15. Li, C., Moro, S., Shostak, K., O'Reilly, F.J., Donzeau, M., Graziadei, A., McEwen, A.G., Desplancq, D., Poussin-Courmontagne, P., Bachellart, T., Fiskin, M., Berrodier, N., Pichard, S., Brillet, K., Orfanoudakis, G., Poterszman, A., Torbeev, V., Rappsilber, J., Davey, N.E., Chariot, A., & Zanier, K. (2024). Molecular mechanism of ikk catalytic dimer docking to nf-κb substrates. Nat Commun, 15, 7692. https://doi.org/10.1038/s41467-024-52076-0
16. Liu, Z., Wang, H., Wu, Y., Bian, S., Ma, J., & Li, X. (2025). Dre-mir-223/ikkα/nf-κb promotes inflammatory response in zebrafish liver (zfl) cells induced by microcystin-lr. Fish Shellfish Immunol, 167, 110689. https://doi.org/10.1016/j.fsi.2025.110689
17. Luan, H., Huo, Z., Zhao, Z., Zhang, S., Huang, Y., Shen, Y., Wang, P., Xi, J., Liang, J., & Wu, F. (2020). Scutellarin, a modulator of mtor, attenuates hepatic insulin resistance by regulating hepatocyte lipid metabolism via srebp-1c suppression. Phytother Res, 34, 1455-1466. https://doi.org/10.1002/ptr.6582

18. Selman, A., Burns, S., Reddy, A.P., Culberson, J., & Reddy, P.H. (2022). The role of obesity a nd diabetes in dementia. Int J Mol Sci, 23, 926 7. https://doi.org/10.3390/ijms23169267
19. Wen, L., He, T., Yu, A., Sun, S., Li, X., Wei, J., Song, R., Yan, X., Li, R., Ren, X., Wang, Y., L iu, X., Dong, Y., Fu, X., & She, G. (2021). Bre viscapine: A review on its phytochemistry, pha rmacokinetics and therapeutic effects. Am J C hin Med, 49, 1369-1397. https://doi.org/10.11 42/S0192415X21500646
20. Xourafa, G., Korbmacher, M., & Roden, M. (2 024). Inter-organ crosstalk during developmen t and progression of type 2 diabetes mellitus. Nat Rev Endocrinol, 20, 27-49. https://doi.org/ 10.1038/s41574-023-00898-1
21. Ye, Z., Ge, Z., Yang, S., Hu, T., Ye, Q., & Che n, H. (2024). Scutellarein alleviates osteoarthri tis progression through the pi3k/akt/nf-kappab signaling pathway: In vitro and in vivo studie s. Phytother Res, 38, 3509-3524. https://doi.or g/10.1002/ptr.8232
22. Younis, N.S., & Ghanim, A.M.H. (2022). The protective role of celastrol in renal ischemia-re perfusion injury by activating nrf2/ho-1, pi3k/ akt signaling pathways, modulating nf-κb sign aling pathways, and inhibiting erk phosphoryl ation. Cell Biochem Biophys, 80, 191-202. htt ps://doi.org/10.1007/s12013-022-01064-6
23. Zhang, W., Song, M., Fang, Z., Chen, F., Yua n, H., Gao, X., & Liu, K. (2024). Role of extra cellular vesicles in insulin resistance: Signalin g pathways, bioactive substances, mirnas, and therapeutic potential. Cell Biochem Funct, 42, e4013. https://doi.org/10.1002/cbf.4013
24. Zhang, X., Dong, Z., Fan, H., Yang, Q., Yu, G., Pan, E., He, N., Li, X., Zhao, P., Fu, M., & Dong, J. (2023). Scutellarin prevents acute alc ohol-induced liver injury via inhibiting oxidati ve stress by regulating the nrf2/ho-1 pathway and inhibiting inflammation by regulating the akt, p38 mapk/nf-κb pathways. J Zhejiang Uni v Sci B, 24, 617-631. https://doi.org/10.1631/j zus.B2200612
25. Zhou, C.-H., Yang, H., Zou, L.-F., Liu, D.-F., Yu, L.-Z., Cao, H.-H., Deng, L.-E., Wang, Z.- W., Lu, Z.-B., & Liu, J.-S. (2023). Ethyl lithos permate reduces lipopolysaccharide-induced i nflammation through inhibiting nf-κb and stat 3 pathways in raw 264.7 cells and zebrafish. C hin J Integr Med, 29, 1111-1120. https://doi.or g/10.1007/s11655-023-3643-y
26. Zhou, X., Zhu, Y., Gao, D., Li, M., Lin, L., Wa ng, Z., Du, H., Xu, Y., Liu, J., He, Y., Guo, Y., Wang, S., Qiao, S., Bao, Y., Liu, Y., & Zhang, H. (2024a). Matrilin-3 supports neuroprotectio n in ischemic stroke by suppressing astrocyte-mediated neuroinflammation. Cell Rep, 43, 11 3980. https://doi.org/10.1016/j.celrep.2024.11 3980
27. Zhou, Y., Gu, C., Zhu, Y., Zhu, Y., Chen, Y., S hi, L., Yang, Y., Lu, X., & Pang, H. (2024b). P harmacological effects and the related mechan ism of scutellarin on inflammation-related dise ases: A review. Front Pharmacol, 15, 1463140. https://doi.org/10.3389/fphar.2024.1463140